UDC 546.72: 54.161: 54.061:54.04:54.03

DOI: 10.15372/CSD20180512

Effect of the Mesoporous Matrix on Thermal Decomposition of Iron (III) Oxalate

P. YU. TYAPKIN[1], S. A. PETROV[1], A. P. CHERNYSHEV[1,2], K. B. GERASIMOV[1], and N. F. UVAROV[1,2,3]

[1]*Institute of Solid State Chemistry and Mechanochemistry, Siberian Branch, Russian Academy of Sciences, Novosibirsk, Russia*

E-mail: p.yu.tyapkin@gmail.com

[2]*Novosibirsk State Technical University, Novosibirsk, Russia*

[3]*Novosibirsk State University, Novosibirsk, Russia*

Abstract

Processes of thermal decomposition of iron (III) oxalate placed into pores of structured mesoporous silica (SBA-15) were investigated. Synchronous thermal analysis of samples was carried out in inert (argon) and oxidizing (a mixture of argon and 20 % oxygen) media. The composition of gas thermolysis products was detected mass spectrometrically. The initial salt and solid-phase products of its decomposition were characterised by X-ray phase analysis and Mössbauer spectroscopy. It is well known that the process of thermolysis of iron (III) oxalate under inert atmosphere conditions proceeds in two stages: intermediate decomposition to anhydrous iron (II) oxalate and then the final one to Fe_3O_4 and α-Fe at 150–180 and 310–400 °C, respectively. Oxidative thermolysis occurs in a single step. In other words, iron (III) oxide is formed from the initial salt that is later crystallised into hematite phase. However, this step is complex. Instantaneous oxidation of anhydrous iron (II) oxalate formed as an intermediate explains high exothermicity of the process. It was found that the temperature of the initial decomposition step was reduced from 150 to 80 °C for a precursor placed into SBA-15 silica matrix pores in both oxidative and inert media. Herewith, the finishing temperature of the step for oxidative thermolysis is increased almost by 100 °C. Gas evolution spikes and extremes in the calorimetric curve of the second step of decomposition in argon are reduced by 30–40 °C. An increase in the reactivity of fine particles and the amorphous state of iron (III) oxalate explained a reduction in gas evolution peaks. In order to describe the behaviour of the precursor, upon oxidative thermolysis likely reactions determining the process were suggested.

Key words: thermolysis, SBA-15, iron (III) oxalate, iron oxides, synchronous thermal analysis, Mössbauer spectroscopy

INTRODUCTION

Mesoporous iron-containing composites are promising materials for the use in the widest areas of human activities, such as medicine [1, 2], environmental measures [3, 4], catalysis [4, 5], *etc.* [6, 7]. Nevertheless, processes occurring upon the preparation of iron oxides nanoparticles by thermolysis of different precursors under conditions of the limited exchange between the precursor and the external medium are rarely considered when exploring properties of such objects. The porous matrix is not only a functional component of the composite produced and limits the particle size of the solid-phase decomposition product of the precursor placed therein but also locally forms the reaction medium that is different from the initially given one.

This aspect is especially critical for precursors, thermolysis of which is accompanied by the for-

mation of a large amount of gaseous products. A typical example of such precursors is iron (III) oxalate. Four moles of carbon dioxide and 2 moles of carbon monoxide are formed from 1 mole of salt upon decomposition in an inert atmosphere:

$$Fe_2(C_2O_4)_3 \cdot xH_2O \rightarrow 2FeC_2O_4 + 2CO_2 + xH_2O \quad (1)$$

$$FeC_2O_4 \rightarrow FeO + CO_2 + CO \quad (2)$$

or 6 moles of CO_2 upon oxidative thermolysis:

$$2FeC_2O_3 + 1.5O_2 \rightarrow Fe_2O_3 + 4CO_2 \quad (3)$$

Anhydrous iron (II) oxalate (FeC_2O_4) is formed as a primary solid-phase product regardless of reaction medium composition upon thermolysis of iron oxalate (III) tetrahydrate ($Fe_2(C_2O_4)_3 \cdot 4H_2O$) [8]. This is linked to electron transfer from the oxalate group ($C_2O_4^{2-}$) towards iron cations upon breaking off a carbon chain. Herewith, there takes place a major nonconformity of the volumes of unit cell volumes for the initial salt and the product: the molar volumes of cell phases $FeC_2O_4 \cdot 2H_2O$ [9] and $Fe_2(C_2O_4)_3 \cdot 4H_2O$ [10] are different in almost 60 % and over (for anhydrous iron (II) oxalate). As a consequence, accumulating structural stresses relaxes *via* the formation of a new surface, which leads to a reduced size of product particles. Multi-step thermolysis may typically set the multilevel hierarchical structure of the product [11]. The shape of the initial, larger particles that now consist of contacting fine species of the new FeC_2O_4 phase is preserved for the system under consideration. Moreover, the final solid-phase thermolysis product is also formed as a pseudomorph [8, 11]. Upon thermolysis in a closed system, the reaction atmosphere is formed due to its own gaseous decomposition products and is able to have an effect on both thermolysis mechanism and phase composition of products. As demonstrated by thermolysis research of iron (II) oxalate under conversion gasses, cementite (Fe_3C) may become apparent in the composition of the solid-phase thermolysis product here [12].

The objective of this research was to explore the effect of the mesostructured silica SBA-15 matrix on thermolysis mechanisms of iron (III) oxalate placed in its inner volume. The initial salt and its thermal decomposition products were analysed by X-ray powder diffraction and Mössbauer spectroscopy for cases of thermolysis of the free matrix and the salt placed into its pores.

MATERIALS AND METHODS

Mesoporous structured silica SBA-15 (a specific surface area of 533 m^2/g) with an ordered hexagonal (an ordering parameter of 10.4 nm) cylindrical pores (with a maximum diameter distribution of 7.4 nm) was presented by the Institute of Chemistry and Chemical Technology, Siberian Branch, Russian Academy of Sciences (Krasnoyarsk). In order to synthesise iron (III) oxalate tetrahydrate according to the equation

$$3H_2C_2O_4 \cdot 2H_2O + 2Fe(OH)_3 = Fe_3(C_2O_4)_3 + 12H_2O \quad (4)$$

chemically pure reagents, such as iron (III) hydroxide ($Fe(OH)_3$) and oxalic acid dihydrate ($H_2C_2O_4 \cdot 2H_2O$), were used. A warm solution of the acid (100 g/L) was poured in small portions to $Fe(OH)_3$ placed into a glass beaker and the contents were continuously stirred. The procedure was carried out until complete dissolution of hydroxide. Afterwards, the solution was dried in a Petri dish at room temperature, having placed the beaker into the dark place in order to avoid photolysis of the compound.

A composite (the sample is designated as FeSBA) was made by impregnation of the matrix with an aqueous solution (30 g/L) of the precursor in an amount of 1 mL of solution per 150 mg of the matrix. In total, three impregnations were performed. The samples were aged in a desiccator after each procedure of this type.

Thermal analysis of the samples in oxidative (80 % of argon and 20 % of oxygen) and inert (argon) media was carried out using a specialised STA 449 F1 Jupiter devise (Netzsch, Germany). The instrument is equipped with a QMS403 C Aeolos mass spectrometer (Netzsch, Germany) to analyse the phase composition of gaseous thermolysis products. Upon surveying in an inert gas medium, heating was carried out with a rate of 5 °C/min, in oxidative one – with 3 °C/min. The total flow rate of gases (Ar or Ar + O_2) was 50 mL/min.

In order to carry out X-ray phase analysis, a D8 Advance X-ray diffraction meter (Bruker, Germany) using CuK_α radiation (λ = 1.5418 Å) was used. Phase identification was carried out by comparison with theoretical X-ray diffraction patterns plotted according to the PDF2 database.

Data regarding the chemical state of iron cations was acquired by Mössbauer ^{57}Fe spectroscopy with a source of ^{57}Co(Rh) γ-quanta. Spectra were taken at room temperature in the transmission geometry, using an NP 255/610 spectrometer (Hungary) with a NZ-640 rate control board. The unit operates in the mode of constant accelerations with rate reverse. Isomeric shifts δ are given in relation to α-Fe metallic iron with an error of ±0.005 mm/s. Determination errors of quadru-

TABLE 1

Results of simultaneous thermal analysis of iron oxalate (III) tetrahydrate in a free state and the species placed in the pores of the silica SBA-15 matrix (FeSBA sample)

Sample	Atmosphere	Temperature range (°C) of release of			Mass loss*, %
		H_2O	CO_2	CO	
$Fe_2(C_2O_4)_3 \cdot 4H_2O$	Ar	100–210	150–200, 310–400	310–400	67.11 (67.91)
	80 % Ar + 20 % O_2	110–180	150–180	–	63.79 (64.34)
FeSBA	Ar	up to 220	80–200, 270–400	270–400	18.7
	80 % Ar + 20 % O_2	up to 220	80–280	–	19.6

* Computed theoretical values are given in brackets.

pole splitting (ΔE_Q) values, hyperfine magnetic fields, and line widths are ±0.01 mm/s, whereas those of relative spectra squares are ±0.1 %.

RESULTS AND DISCUSSION

The X-ray diffraction pattern of the FeSBA sample does not have typical Bragg reflexes of the iron (III) oxalate phase. There is a wide low-intensity halo of the matrix.

As indicated by analysis of Mössbauer spectra of the samples, there are high-spin Fe^{3+} cations in octahedral surroundings. Spectral parameters of a free precursor ($\delta = 0.378$ mm/s and $\Delta E_Q = 0.45$ mm/s) correspond to literature data [10], whereas characteristics of the FeSBA sample ($\delta = 0.396$ mm/s and $\Delta E_Q = 0.61$ mm/s) are typical for amorphous iron (III) oxalate [13]. As it follows from the analysis of Mössbauer spectra of solid products of thermolysis of iron (III) oxalate placed into matrix pores, Fe^{3+} iron cations are found in two states. The component with the quadrupole splitting parameter $\Delta E_Q = 0.67–0.68$ mm/s is assigned to the ferrihydrite phase, and the one with $\Delta E_Q = 1.14–1.18$ mm/s to amorphous iron (III) oxide [8, 14, 15]. The quantitative ratio between iron cations belonging to the first and second components for the product of oxidative thermolysis is about 7 : 3, whereas that for decomposition in an inert atmosphere – 4 : 6.

Table 1 presents the results of synchronous thermal analysis of all samples. Figures 1 and 2 give ion currents and sample relative mass, respectively, *vs* temperature. Dehydration of the initial oxalate begins at 100–110 °C. Water release continues as high as 210 or 180 °C in an inert (Ar) or oxidizing (Ar + 20 % O_2) atmospheres, respectively. Decomposition in an inert medium proceeds in two stages: in the 150–200 °C range (reaction (1)) with the release of CO_2 and within 310–400 °C according to reactions (2) and

$$4FeO \rightarrow Fe_3O_4 + \alpha\text{-}Fe \qquad (5)$$

to yield CO *и* CO_2.

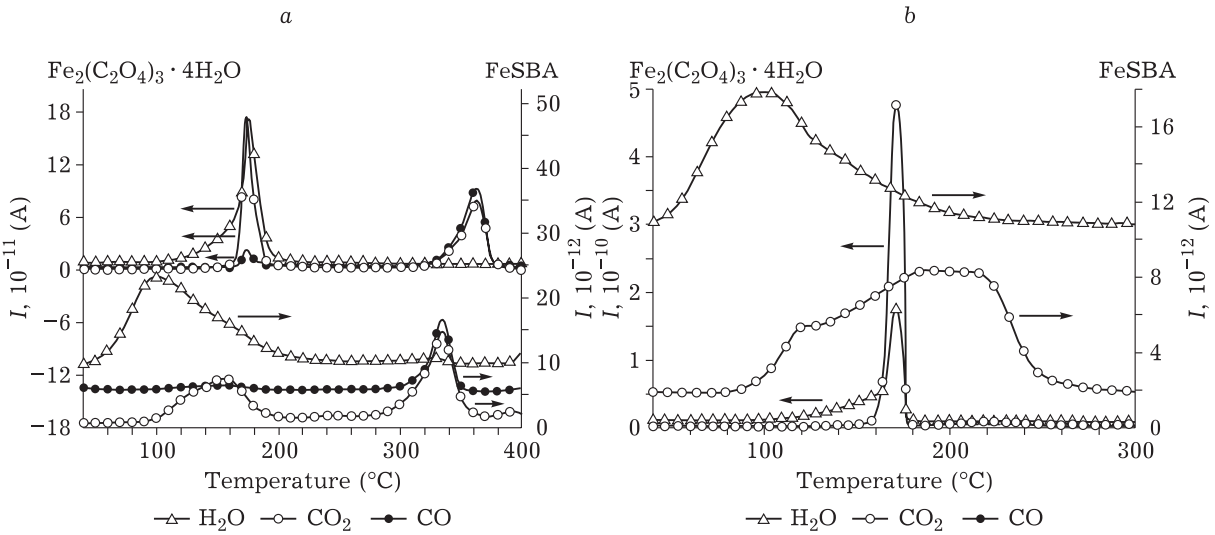

Fig. 1. Mass spectrometric phase analysis of gaseous products released upon thermolysis of samples $Fe_2(C_2O_4)_3 \cdot 4H_2O$ and FeSBA in argon (*a*) and a mixture of 80 % Ar + 20 % O_2 (*b*).

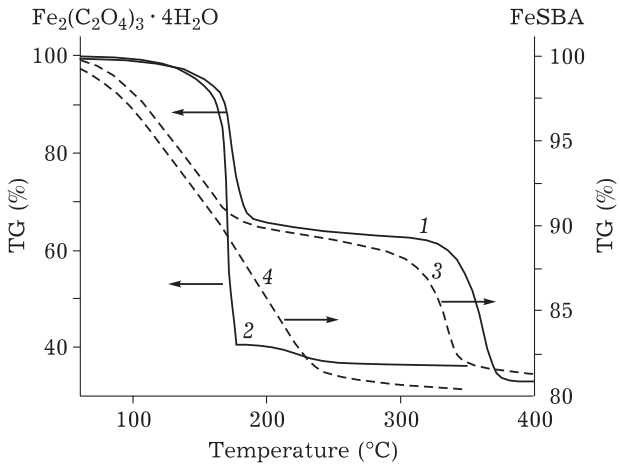

Fig. 2. TG curves of the $Fe_2(C_2O_4)_3 \cdot 4H_2O$ precursor and the FeSBA sample decomposed in argon (*1*, *3*) and a mixture of 80 % Ar + 20 % O_2 (*2*, *4*).

X-ray phase analysis of the solid product detected magnetite (Fe_3O_4), maghemite (γ-Fe_2O_3) and iron metal (α-Fe) phases (Fig. 3).

In the oxidizing medium, thermolysis occurs as a single step, however, a complex procedure consisting of reactions (1) and (3). The process proceeds in the 150–180 °C temperature range. Apart from water, carbon dioxide is released as a gaseous product of thermolysis. The X-ray diffraction pattern of the solid product contains at least two clearly visible broad reflexes near 2θ = 35 and 63° positions. This picture is ascribed to ferrihydrite ($5Fe_2O_3 \cdot 8H_2O$) or hydrated poorly crystallized Fe_2O_3 [16].

The final product of decomposition of iron (III) oxalates in the oxygen-containing medium is usually hematite. However, magnetite or maghemite phases may also be detected at certain conditions (low oxygen content, high heating rate, and large sample thickness). Nevertheless, initially formed fine particles of several nanometers in size form the ferrihydrite phase that is transformed into other oxides upon particles enlarging and water desorption.

The nature of thermolysis is somewhat different for the precursor placed into matrix pores. First of all, onset temperatures of decomposition steps and peak positions of gas release are reduced by several dozens of degrees (see Table 1). This is likely related to an increase in the reactivity of iron oxalates particles when increasing their dispersity and perhaps, to a decrease in the activation temperature of the process due to the interaction with the matrix. We believe that a shift of the first step of decomposition may be related to the presence of iron (III) oxalate as a metastable amorphous phase.

The finishing temperature of decomposition steps for thermolysis in an inert atmosphere remains constant. We do not tend to assume a substantial change in the mechanism of salt decomposition in this case. Nevertheless, the metallic iron phase was not detected in solid-phase products. The progression of the reaction at elevated carbon dioxide pressure developed by the matrix may explain this phenomenon:

$$3FeO + CO_2 \rightarrow Fe_3O_4 + CO \qquad (6)$$

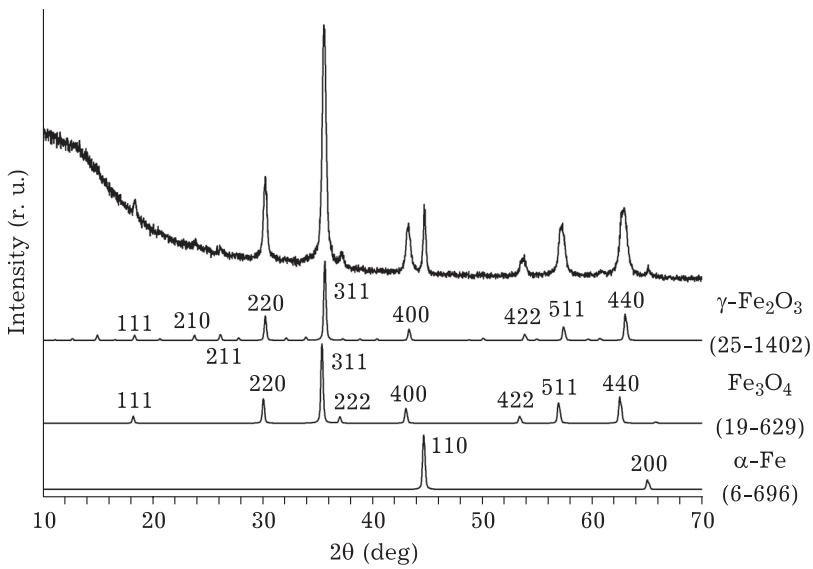

Fig. 3. X-ray phase analysis of the thermolysis product of iron (III) oxalate tetrahydrate ($Fe_2(C_2O_4)_3 \cdot 4H_2O$) under argon. Theoretical X-ray diffraction patterns were plotted according to the PDF-2 database.

Thermolysis of iron (III) oxalate placed into SBA-15 matrix pores proceeds under oxidative conditions and is notable for a decrease in the onset temperature of the reaction, a noticeable increase in the finishing temperature (by 100 °C), and a plateau-like type of areas of the curve of releasing gas (CO_2). A low oxygen advance speed towards the reaction zone (the reaction flows in matrix pores, which limits the exchange of matter with the external medium) and also the rate of flow of energy evolved upon salt oxidation for evaporation of matrix-absorbed water make it possible to partially divide steps of formation and decomposition (reactions (1) and (3), respectively) of anhydrous iron (II) oxalate. The presence of two plateaus of different heights may be explained on the assumption of pore capping with trivalent salt. As decomposition of iron (III) oxalate progresses, the pores become empty, whereas the rate of carbon dioxide removal is increased. Reactions (2) and (5) become likely under oxygen shortage condition, however, ferrihydrite remains the final thermolysis product.

CONCLUSION

The effect of the mesostructured silica SBA-15 matrix on thermolysis mechanisms of iron (III) oxalate placed in its inner volume has been explored. It has been determined that onset temperatures of decomposition reactions in an inert (Ar) and oxidative (Ar + 20 % O_2) media were reduced by several dozens of degrees, apparently due to the reactivity enhancement of fine particles of salt and the interaction with the matrix.

The interaction of wustite ($Fe_{1-x}O$) and CO_2 formed during the decomposition of anhydrous iron (II) oxalate, with which the lack of metallic iron in the solid-phase thermolysis product is related to, is likely upon thermolysis in mesopores under an inert atmosphere. The upper boundary of the reaction temperature range is increased by 100 °C in the oxidizing medium due to difficulties in the removal of CO_2 released upon thermolysis of iron (III) ferrioxalate and oxygen ingress. Herewith, reactions typical for thermolysis under inert conditions are not excluded. Phases of ferrihydrite and amorphous iron (III) oxide become apparent in the composition of the solid-phase thermolysis product in both cases.

It has been found that Mössbauer spectral parameters (isomer shifts and quadrupole splitting) of amorphous phase samples of iron (III) oxalate are similar to those of specimens produced by impregnation of mesoporous silica with an aqueous solution of iron (III) oxalate. And that is what indicates the stabilization of the amorphous state of iron (III) oxalate hydrate in matrix pores.

REFERENCES

1 Soltys M., Kovacik P., Lhotka M., Ulbrich P., Zadrazil A., Stepanek F., *Micropor. Mesopor. Mater*. 2016. Vol. 229. P. 14–21.
2 Wang P. F., Jin H. X., Chen M., Jin D. F., Hong B., Ge H. L., Gong J., Peng X. L., Yang H., Liu Z. Y., Wang X. Q., *J. Nanomaterials*. Vol. 2012. Article ID: 269861. 7 p.
3 Huang H., Ji Y., Qiao Z., Zhao Ch., He J., Zhang H., *J. Automated Methods and Management in Chemistry*. 2010. Article ID: 323509. 7 p.
4 Li Y., Guan Y., van Santen R. A., Kooyman P. J., Dugulan I., Li C., Hensen E. J. M., *J. Phys. Chem. C*. 2009. Vol. 113, No. 52. P. 21831–21839.
5 Mazilu I., Ciotonea C., Chirieac A., Dragoi B., Catrinescu C., Ungureanu A., Petit S., Royer S., Dumitriu E., *Micropor. Mesopor. Mater*. 2017. Vol. 241. P. 326337.
6 Kharlamova M. V., Sapoletova N. A., Eliseev A. A., Lukashin A. V., *Tech. Phys. Lett*. 2008. Vol. 34, No. 7. P. 36–43.
7 Yoon T. J., Yu K. N., Kim E., Kim J. S., Kim B. G., Yun S.-H., Sohn B.-H., Cho M.-H., Lee J.-K., Park S. B., *Small*. 2006. Vol. 2, No. 2. P. 209–215.
8 Hermankova P., Hermanek M., Zboril R., *Eur. J. Inorg. Chem*. 2010. P. 1110–1118.
9 Echigo T., Kimata M., *Phys. Chem. Miner*. 2008. Vol. 35. P. 467–475.
10 Ahouari H., Rousse G., Rodriguez-Carvajal J., Sougrati M.-T., Saubanere M., Courty M., Recham N., Taarscon J.-M., *Chem. Mater*. 2015. Vol. 27 (5). P. 1631–1639.
11 Cherepanova S. V., Ancharova U. V., Vulavchenko O. A., Venediktova O. S., Gerasimov E. YU., Leont'eva N. N., Matvienko A. A., Maslennikov D. V., Pakharukova V. P., Sidel'nikov A. A., Tsybulya S. V., Chizhik S. A., Yatsenko D. A. Nanostrukturirovannye oksidy. Novosibirsk: IPTS NGU, 2016. 206 p.
12 Hermanek M., Zboril R., Mashlan M., Machala L., Schneeweiss O., *J. Mater. Chem*. 2006. Vol. 16, Is. 13. P. 1273–1280.
13 Tyapkin P. Yu., Petrov S. A., Chernyshev A. P., Ancharov A. I., Sheludyakova L. A., Uvarov N. F., *Journal of Structural Chemistry*. 2016. Vol. 57, No. 6. P. 1134–1140.
14 Zboril R., *Chem. Mater*. 2002. Vol. 14. P. 969 –982.
15 Tyapkin P. Yu., Petrov S. A., Chernyshev A. P., Larichev Yu. V., Kirik S. D., Gribov P. A., Uvarov N. F., *Mater. Today: Proc*. 2017. Vol. 4(11). P. 11392–11395.
16 Chappell H. F., Thom W., Bowron D. T., Faria N., Hasnip Ph. J., Powell J. J., *Phys. Rev. Materials*. 2017. Vol. 1(3). Article ID: 036002. 8 p.